Cell Host & Microbe
Short Article

Platelet Factor 4 Activity against *P. falciparum* and Its Translation to Nonpeptidic Mimics as Antimalarials

Melissa S. Love,[1,8] Melanie G. Millholland,[1,8] Satish Mishra,[4] Swapnil Kulkarni,[1] Katie B. Freeman,[5] Wenxi Pan,[5] Robert W. Kavash,[5] Michael J. Costanzo,[5] Hyunil Jo,[2] Thomas M. Daly,[6] Dewight R. Williams,[3] M. Anna Kowalska,[7] Lawrence W. Bergman,[6] Mortimer Poncz,[7] William F. DeGrado,[2] Photini Sinnis,[4] Richard W. Scott,[5] and Doron C. Greenbaum[1,*]
[1]Department of Pharmacology
[2]Department of Biochemistry and Molecular Biophysics
[3]Department of Pathology and Laboratory Medicine
University of Pennsylvania, Philadelphia, PA 19104, USA
[4]Department of Molecular Microbiology and Immunology, Johns Hopkins Bloomberg School of Public Health, Baltimore, MD 21205, USA
[5]PolyMedix, Inc., Radnor, PA 19087, USA
[6]Department of Microbiology and Immunology, Drexel University College of Medicine, Philadelphia, PA 19129, USA
[7]Department of Pediatrics, Children's Hospital of Philadelphia, Philadelphia, PA 19104, USA
[8]These authors contributed equally to this work
*Correspondence: dorong@upenn.edu
http://dx.doi.org/10.1016/j.chom.2012.10.017

SUMMARY

Plasmodium falciparum pathogenesis is affected by various cell types in the blood, including platelets, which can kill intraerythrocytic malaria parasites. Platelets could mediate these antimalarial effects through human defense peptides (HDPs), which exert antimicrobial effects by permeabilizing membranes. Therefore, we screened a panel of HDPs and determined that human platelet factor 4 (hPF4) kills malaria parasites inside erythrocytes by selectively lysing the parasite digestive vacuole (DV). PF4 rapidly accumulates only within infected erythrocytes and is required for parasite killing in infected erythrocyte-platelet cocultures. To exploit this antimalarial mechanism, we tested a library of small, nonpeptidic mimics of HDPs (smHDPs) and identified compounds that kill *P. falciparum* by rapidly lysing the parasite DV while sparing the erythrocyte plasma membrane. Lead smHDPs also reduced parasitemia in a murine malaria model. Thus, identifying host molecules that control parasite growth can further the development of related molecules with therapeutic potential.

INTRODUCTION

Malaria is a devastating disease and continues to be a global health burden, causing significant morbidity and mortality (Gething et al., 2011). The pathogenesis of malaria is modulated both positively and negatively by many human cell types in blood, including monocytes, neutrophils, and platelets (Goodier et al., 1995; Pain et al., 2001). Recently, platelets have been shown to bind infected erythrocytes and kill intracellular malaria parasites (McMorran et al., 2009). Previous studies have suggested that thrombocytopenia is a poor prognostic marker in malaria (Moerman et al., 2003) and is associated with cerebral malaria (Wassmer et al., 2008). We therefore pursued the hypothesis that host cells found in the bloodstream that are known to secrete proteins with host defense peptide (HDP) activity (Tang et al., 2002) could contribute to the host's control of malaria parasite proliferation in the blood stage.

HDPs play a central role in the innate immune system (Finlay and Hancock, 2004; Hancock and Lehrer, 1998; Tossi et al., 2000; Zasloff, 2002). HDPs display broad-spectrum action against bacteria, fungi, protozoa, and viruses, which has promoted their use as leads for developing antibiotics (Zasloff, 2002). A unifying characteristic of HDPs is an amphipathic topology in which the cationic and hydrophobic side chains segregate onto opposing faces of the overall folded molecule. It is thought that the physicochemical properties of HDPs, rather than any specific sequence or structure, are responsible for their activities. HDPs are thought to bind the membrane surface in a noncooperative fashion and then aggregate once a threshold concentration is reached, causing membrane permeabilization (Christensen et al., 1988; Ludtke et al., 1995). It is believed that amphipathic topology is essential for insertion into and disruption of membranes, leading to pathogen death. From this background, we hypothesized that naturally occurring bloodstream HDPs, especially from platelets, might have the ability to kill *P. falciparum* early in erythrocytic infection.

RESULTS

Identification of hPF4 as an Antiparasitic HDP that Kills *P. falciparum* via Lysis of the Parasite DV

A screen of HDPs found in the bloodstream, secreted by a variety of cells including platelets, neutrophils, and lymphocytes, was performed to assess their antiparasitic activity (Figure 1A). This screen revealed that several proteins killed *P. falciparum*

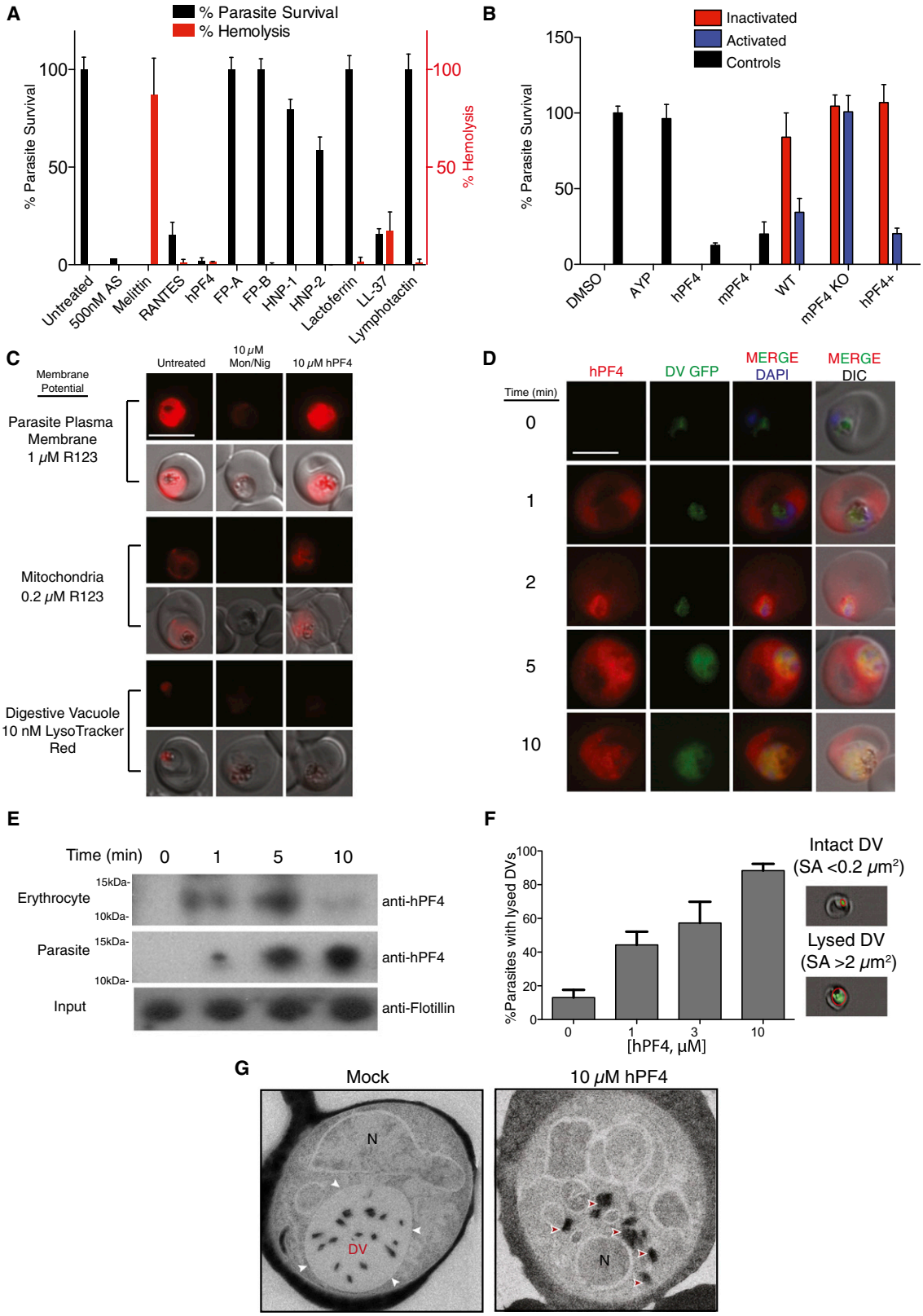

Figure 1. hPF4 Acts as a HDP against *P. falciparum* via Lysis of the Parasite DV

(A) Screen of human HDPs found in blood for *P. falciparum* killing and hemolysis at 15 μM, including Regulated upon Activation, Normal T cell Expressed, and Secreted (RANTES); hPF4; Fibrinopeptide-A (FP-A); Fibrinopeptide-B (FP-B); Human Neutrophil Peptides 1 and 2 (HNP-1; HNP-2); and Cathelicidin (LL-37).

in vitro without affecting the host erythrocyte. Most notably, hPF4 showed high potency against *P. falciparum* with an IC_{50} of 4.2 μM and no significant hemolysis. Considering local concentrations of hPF4 have been reported to reach at least 280 μM surrounding activated platelets (Kowalska et al., 2010), the antiparasitic IC_{50} of hPF4 has in vivo relevance. Platelets harvested from wild-type (WT), mouse PF4 (mPF4) knockout (mPF4 KO), or overexpressing hPF4 ($hPF4^+$) mice were tested against *P. falciparum* in culture with recombinant mPF4 and hPF4 as controls (Figure 1B). Because there is no evidence to suggest that mouse platelets bind to or are activated by human infected erythrocytes, platelets were preactivated with AYP prior to their addition to parasite cultures. Preactivated WT and $hPF4^+$ mouse platelets were able to kill *P. falciparum* in culture, while littermate PF4 KO platelets showed no killing capacity. Thus it appears that PF4 is a major antimalarial component of activated platelets.

As membrane perturbation is an established mechanism of action for HDPs (Bechinger, 2009; Westerhoff et al., 1989), we examined the integrity of potential target parasite membranes upon hPF4 treatment. Since hPF4 had little hemolytic capability, we reasoned the erythrocyte integrity was not significantly compromised. Parasite plasma membrane (PPM) potential assays showed no discernible loss of potential following 4 hr of hPF4 exposure (Figure 1C). Next, the integrity of established intracellular organelle targets, including the mitochondria and lysosome-like digestive vacuole (DV), was assessed post-hPF4 treatment. Analysis of membrane potential revealed no perturbation of the mitochondria; however, a significant loss of proton potential was observed in the DV within minutes of treatment (Figure 1C). To further investigate this DV perturbation, transgenic parasites expressing green fluorescent protein (GFP)-tagged plasmepsin-II in the DV (Klemba et al., 2004) were treated with hPF4 and followed by fluorescence microscopy over a 10 min time course. Parasites were assayed for both hPF4 localization using immunofluorescence analysis (IFA) and direct GFP signal (integrity of the DV; Figure 1D). Within 1 min of hPF4 incubation, hPF4 staining could be detected in the cytoplasm of only infected erythrocytes. hPF4 continued to accumulate over the next several minutes, wherein it entered the parasite cytoplasm and colocalized with the parasite DV. Next, severe perturbation of the DV allowed GFP to diffuse throughout the parasite cytoplasm (Figure 1D, Figures S1A and S1B). Western blot analysis of hPF4 confirmed the IFA results showing entry into erythrocytes by 1 min followed by accumulation into the parasite within 5 min (Figure 1E). To assess the loss of DV integrity on the population level, we utilized quantitative flow cytometry to first capture images of individual parasite-infected cells, then quantitatively differentiate based on DV fluorescent surface area (SA) intact DVs (<0.2 $\mu m^{2)}$ from lysed DVs (>2 μm^2; Figure 1F, Figure S1C). hPF4 treatment caused dose-dependent DV lysis, with nearly complete DV lysis on a population level upon exposure to 10 μM hPF4. The loss of DV integrity was confirmed at high resolution using transmission electron microscopy imaging to compare untreated and hPF4-treated parasites, revealing the complete loss of DV integrity in the hPF4-treated parasites versus mock-treated parasites with a clearly delineated DV membrane (white arrowheads; Figure 1G, also see Movie S1). In addition to the loss of DV organellar structure, hemozoin crystals were seen dispersed throughout the parasite (red arrowheads). Thus, DV lysis appears to be the primary mechanism of hPF4 action against parasites. Parasite stages that rely heavily on DV function were especially susceptible to hPF4 treatment (Figure S1E).

The HDP-like C Terminus of hPF4 Has Antiparasitic Activity

hPF4 is comprised of three domains: an N-terminal chemokine domain, a central domain responsible for homotetramerization, and a C-terminal amphipathic helical region with HDP activity (Yeaman et al., 2007). To test the hypothesis that the HDP-like C terminus has activity against the malaria parasite, the 12-residue domain (C12, Figure 2A) was synthesized and tested against *P. falciparum* in vitro (Figure 2B). C12 acted similarly to the parental protein causing loss of parasite DV integrity, was not hemolytic, and did not perturb the PPM or mitochondrial membrane potential after a 4 hr treatment (Figure 2D). Treatment of PM-II-GFP parasites with 100 μM C12 led to leakage of GFP into the parasite cytoplasm following 30 min of exposure, indicating loss of DV integrity (Figure 2E, Figure S2A). In order to ascertain localization of C12 upon treatment, we synthesized a fluorescent version of C12 (C12-TAMRA). Figure 2F shows

Parasite survival was normalized to an untreated control. Artesunate (500 nM) and the HDP melittin (15 μM) were used as positive controls for parasite death without and with hemolysis, respectively. Data shown are means ± SEM.

(B) Parasite-infected erythrocytes were incubated for 24 hr with 2.5×10^8 platelets from either littermate WT, PF4 KO, or $hPF4^+$ mice in the presence or absence of 5 μM AYP to induce platelet activation. Parasite survival was assayed by flow cytometry using SYTOX green as a measurement of DNA content and normalized to an untreated control. Recombinant hPF4 and mPF4 (10 μM) were used as positive controls. Data shown are means ± SEM.

(C) Parasite-infected erythrocytes preincubated with rhodamine 123 (1 μM for parasite plasma membrane potential; 0.2 μM for mitochondrial potential) or 10 nM LysoTracker Red and then treated over a 4 hr time course with 10 μM PF4 or a 10 μM mixture of ionophores Monensin and Nigericin (Mon/Nig). Length bar is 10 μm in each figure.

(D) hPF4 accumulates in the infected erythrocyte cytoplasm prior to lysis of the DV by immunofluorescence. Erythrocytes infected with parasites expressing plasmepsin-II-GFP (PM-II-GFP) were treated with 1 μM hPF4 over a 10 min time course. Within 1 min of PF4 incubation, PF4 staining is seen in the cytoplasm of infected erythrocytes until entering and inducing lysis of the parasite DV, as shown by GFP signal diffusion through the entire parasite cytoplasm. (Green, PM-II-GFP [DV]; red, hPF4 IFA; blue, parasite nuclei.)

(E) Western blot analysis of erythrocyte fractions or parasite lysates shows early accumulation of hPF4 in infected erythrocytes, followed by persistence in the parasite.

(F) ImageStream flow cytometry shows a dose-dependent increase in PM-II-GFP parasites with a fluorescence surface area of >2 μm^2, an indication of DV lysis, upon treatment with hPF4. Intact DVs have fluorescent surface areas <0.2 μm^2. Data shown are means ± SEM (*$p < 0.05$, **$p < 0.01$).

(G) TEM images reveal dissolution of the DV membrane upon treatment with 10 μM PF4, as well as dispersal of hemozoin fragments throughout the cytoplasm (red arrowheads). Mock-treated controls showed complete integrity of the DV membrane (white arrowheads), encapsulating all hemozoin crystals. (N: parasite nucleus). See also Figure S1 and Movie S1.

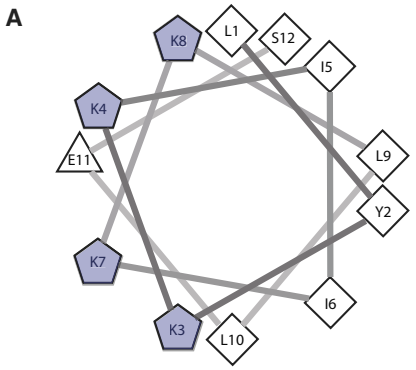

B

Peptide	Sequence	# of K→A	IC_{50} (μM)
PF4	–	–	4.2 ± 0.6
C12	LY^{3}K^{4}KII^{7}K^{8}KLLES	0	73.3 ± 8.1
C12 A3	LY**A**KIIKKLLES	1	84.0 ± 10.8
C12 A3,4	LY**AA**IIKKLLES	2	92.1 ± 16.3
C12 A3,4,7	LY**AA**II**A**KLLES	3	>200
C12 A3,4,7,8	LY**AA**II**AA**LLES	4	Not tested

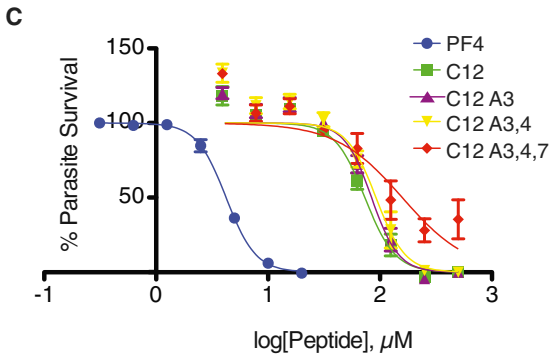

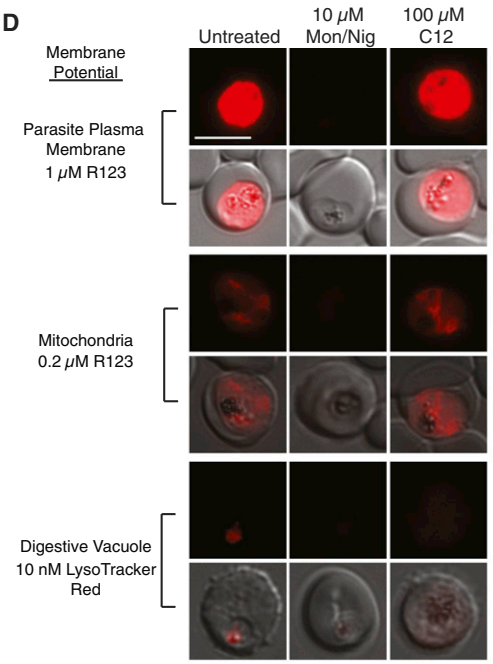

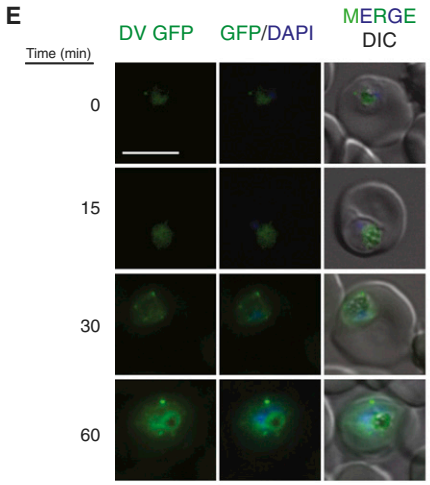

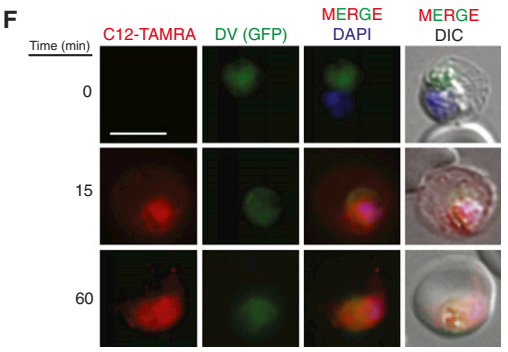

Figure 2. The C-Terminal Amphipathic Helical Domain of PF4 Retains the HDP Activity against *P. falciparum*

(A) Projected helical wheel of C12 with each amino acid numbered.

(B) Peptide derivatives of the PF4 C-terminal domain with lysine residues mutated to alanines to determine the necessity of positive charges for C12 antimalarial activity. Mutated residues are denoted by "A" followed by the residue number. IC_{50}s are means ± SEM (n = 3).

(C) Dose-response curves for PF4, C12, and the series of C12 lysine mutants. Data shown are means ± SEM.

(D) Parasite plasma membrane, mitochondrial, and DV potential were examined upon C12 treatment (see Figure 1B for details).

(E) C12-treated PM-II-GFP parasites showed loss of DV integrity (green, PM-II-GFP [DV]; blue, parasite nuclei.)

(F) C12-TAMRA treatment of PM-II-GFP parasites shows accumulation within infected erythrocytes and parasite bodies within 15 min of exposure, followed by DV lysis within 60 min of treatment. See also Figure S2.

that C12-TAMRA entered only infected erythrocytes within 15 min of treatment, with accumulation in the parasite body and the erythrocyte cytoplasm, while the DV remained intact. Within 60 min of treatment, GFP signal permeated throughout the parasite body, indicating lysis of the DV. As the cationic amphipathicity of HDPs is thought to be key to their mechanism of action, we reasoned that lowering the number of charges on C12 would adversely affect its activity. Starting at the N terminus, mutation of the first or the first two of the four lysines caused only a minor decrease in activity (IC_{50} values of 84.0 μM and 92.1 μM, respectively), while mutation of the first three lysines ablated the antiparasitic activity of C12 (IC_{50} of > 200 μM; Figures 2B and 2C). The quadruple mutant was not tested due to its insolubility. These data suggest that, like most HDPs, activity of the amphipathic C12 peptide is dependent on a minimal cationic charge density.

Synthetic Small Molecule HDP Mimics Are Potent against *P. falciparum* and Have a Mechanism Similar to hPF4

Given their broad activity, HDPs appear to be ideal therapeutic agents, though significant pharmaceutical issues have severely hampered clinical progress, including poor tissue distribution, systemic toxicity, and difficulty and expense of manufacturing (Easton et al., 2009). In addition, PF4 has been reported to worsen experimental cerebral pathology in mice, presumably mediated through the chemokine domain (Srivastava et al., 2008). Thus, we reasoned that synthetic small molecules capable of adopting amphipathic secondary structures analogous to a HDP could potentially reproduce the potent, selective antiparasitic activity of PF4 while improving tissue distribution and decreasing complications arising from chemokine signaling. In addition, these small molecule HDP mimics (smHDPs) are significantly less expensive to produce (an example scaffold is shown in Figure 3A). In order to exploit the DV lysis mechanism of PF4 in a drug discovery effort, a library of ~1,000 nonpeptidic smHDPs (Scott et al., 2008) was tested against *P. falciparum*. A total of 132 compounds were determined to be initial "hits" (14.3% hit rate), using a cutoff of 80% parasite death at 1 μM ($Z' = 0.720$; Figure 3B). Seventy-four compounds were selected for follow-up IC_{50} determination (PMX004-1120, Table S1). Based on these hits, additional compounds were synthesized (PMX1154-1422, Table S1), and seven structurally diverse compounds were chosen as "leads" based on high potency against *P. falciparum*, low hemolytic potential (Figure S3A), and low mammalian cell cytotoxicity. These lead compounds also showed similar potency across a panel of chloroquine-sensitive (3D7, HB3) and chloroquine-resistant (Dd2, 7G8, K1) parasite lines (Figure 3C). Several of the lead compounds displayed little activity against Gram-positive and Gram-negative bacteria and mammalian cells, indicating that a high level of specificity can be built into these nonpeptidic scaffolds. Secondarily, specificity can also be found between simple single-cell eukaryotic pathogens and mammalian cells (Figure 3D). Although all lead compounds showed a similar mechanism of action as PF4, based on acute animal tolerability studies, PMX1207 and PMX207 were selected for more rigorous mechanistic analysis (structures shown in Figure 3E).

Treatment of *P. falciparum* parasites with either PMX1207 or PMX207 disrupted DV membrane potential within 15 min of treatment but did not disturb the PPM or mitochondrial potential, even after 4 hr treatment (Figure 4A). In addition, treatment of the transgenic PM-II-GFP parasites with PMX1207 and PMX207 resulted in rapid diffusion of GFP through the parasite cytoplasm, indicating a catastrophic loss of DV membrane integrity in a manner similar to that observed for hPF4 (Figure 4B; other five leads shown in Figure S4A). Quantitative flow cytometry analysis indicated a dose-dependent effect on DV lysis, with nearly complete DV lysis within the treated population upon treatment with 1 μM of PMX207 or PMX1207 (Figure 4C). We further investigated the intracellular localization and distribution of the smHDPs using PMX496, a potent smHDP with intrinsic fluorescence. PMX496 appeared to accumulate in the parasite body within 30 s, then concentrated in the DV at 1 min, prior to dissipation throughout the parasite body, indicating a loss of DV membrane integrity (Figure S4B). Since cationic amphipathicity is predicted to be necessary for smHDP antiparasitic action, an uncharged isosteric analog of PMX496 was synthesized (PMX1269, $IC_{50} > 2.5$ μM; structures in Figure S4C). As expected, treatment with the uncharged analog did not result in DV lysis, as with the triple alanine C12 mutant. High-resolution transmission electron microscopy and 3D tomograms revealed a complete loss of integrity of the DV after treatment with either PMX1207 or PMX207 (Figure 4D, Movie S2). In addition to free hemozoin crystals (red arrowheads), images showed an accumulation of undigested hemoglobin-containing vesicles (yellow arrowheads; Figure 4D, Figure S4F). Mock-treated parasites showed clear delineating DV membranes (white arrowheads). DV lysis and killing was also evident in Texas Red Dextran-loaded erythrocytes infected with either trophozoite-stage parasites (Figure S4D) or gametocytes (Figure S4E). Loss of gametocyte DV integrity would likely result in parasite death and indicates that smHDPs may have transmission-blocking potential. To further assess the antimalarial capacity of PMX207 and PMX1207, they were screened against an additional five *P. falciparum* isolates encompassing a diverse set of malaria-endemic regions and antimalarial drug resistance characteristics (Figure S3B). All lines were comparably susceptible to these smHDPs, reiterating their potential as antimalarials.

HDP and smHDP Activity Reduce Parasitemia in a Murine Malaria Model

We next tested PF4 and its HDP domain C12 in a non-experimental cerebral malaria (non-ECM) murine malaria model using the 4 day Peters' suppression test (Knight and Peters, 1980). mPF4 treatment significantly reduced parasitemia by 4-fold, while the HDP domain C12 reduced parasitemia by 3-fold (Figures S1F and S2B), indicating that the HDP domain retained antimalarial activity during disease stages in vivo, aside from cerebral malaria. In an ECM model (*P. berghei* ANKA), C12 reduced parasitemia compared to controls on day 5; however, by day 7 (3 days after cease of treatment), parasitemia in the C12-treated mice were significantly higher than controls (Figure S2C). These data suggest that even the C12 domain of PF4 has some immunomodulatory activity that has a negative impact on survival in the *P. berghei* ANKA model of cerebral malaria; therefore, we felt that that the smHDPs have the best potential as antimalarials.

In order to further explore the antimalarial properties of lead smHDPs, PMX207 and PMX1207 were assessed for their ability

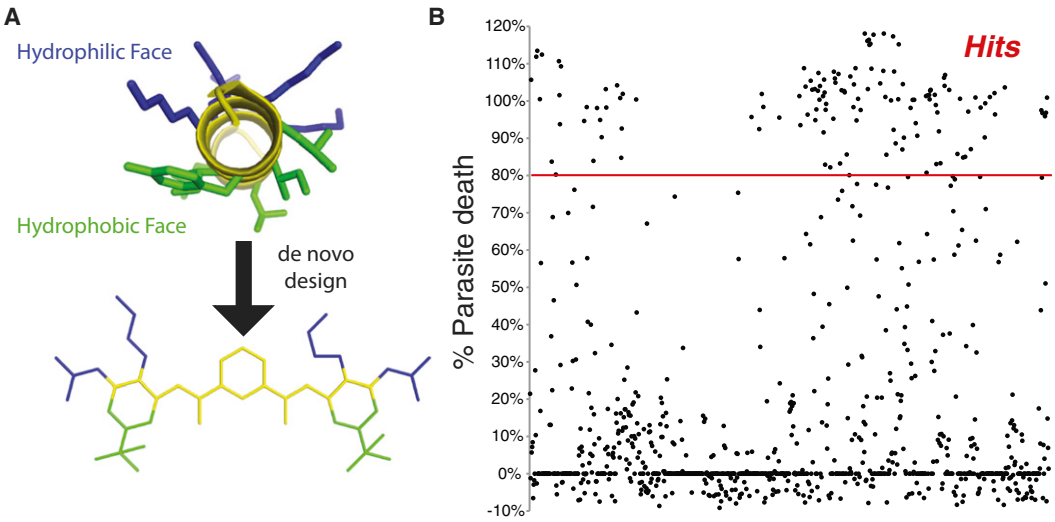

C

Compound	CQ-sensitive *P. falciparum* 3D7 IC_{50} (nM)	CQ-sensitive *P. falciparum* HB3 IC_{50} (nM)	CQ-resistant *P. falciparum* Dd2 IC_{50} (nM)	CQ-resistant *P. falciparum* 7G8 IC_{50} (nM)	CQ-resistant *P. falciparum* K1 IC_{50} (nM)	Mammalian Cells 3T3 EC_{50} (μM)	Mammalian Cells HepG2 EC_{50} (μM)
Chloroquine	8.7 ± 3.3	8.7 ± 1.0	24.6 ± 2.7	37.0 ± 5.8	47.1 ± 6.0	-	-
PMX611	60 ± 20	26 ± 8	49 ± 14	66 ± 14	57 ± 10	769	830
PMX1207	110 ± 12	104 ± 20	75 ± 11	91 ± 7	83 ± 4	65.1	165
PMX207	153 ± 13	133 ± 13	134 ± 10	104 ± 9	95 ± 13	463	536
PMX496	160 ± 60	150 ± 70	170 ± 70	160 ± 60	170 ± 70	139	80
PMX504	160 ± 60	160 ± 60	118 ± 16	113 ± 15	170 ± 70	322	356
PMX647	160 ± 60	170 ± 70	300 ± 100	300 ± 100	610 ± 66	284	433
PMX835	220 ± 50	200 ± 70	300 ± 100	200 ± 70	200 ± 70	>1000	>1000

D

Compound	*Pf* IC_{50} (μg/mL)	*Ec* MIC (μg/mL)	*Sa* MIC (μg/mL)	*Ef* MIC (μg/mL)	*Pa* MIC (μg/mL)	*Kp* MIC (μg/mL)
PMX611	0.032	>50	12.5	25	>50	>50
PMX1207	0.089	0.78	0.78	0.78	6.25	12.5
PMX207	0.17	>50	>50	50	>50	>50
PMX496	0.093	50	50	50	>50	>50
PMX504	0.12	>50	12.5	25	>50	>50
PMX647	0.14	>50	50	25	>50	>50
PMX835	0.20	25	12.5	25	>50	50

E

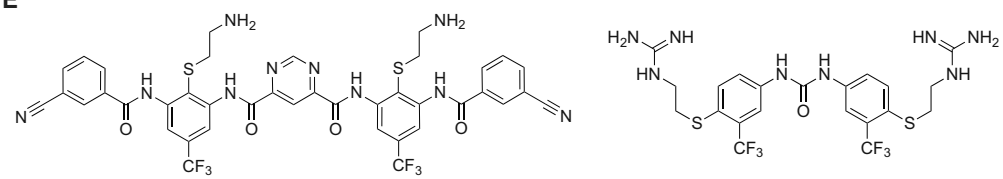

Figure 3. Screen of smHDPs Reveals Potent Inhibitors of *P. falciparum* Growth

(A) Conceptual design of smHDPs from HDPs. Top: Amphipathic structure of magainin 2; cationic groups in blue, nonpolar groups in green, peptide backbone in yellow. Bottom: de novo designed smHDPs capture the facially amphipathic architecture and critical physicochemical properties needed to establish robust antimicrobial activity.

(B) Screen of 920 smHDPs at 500 nM against *P. falciparum*. Parasite death was normalized to a chloroquine control (14.3% hit rate, Z′ = 0.720).

(C) Lead smHDPs were screened against a panel of chloroquine-sensitive and chloroquine-resistant *P. falciparum* lines. Chloroquine was used as a positive control for parasite death. IC_{50}s are as mean ± SEM, n > 3 for each compound. Cytotoxicity (EC_{50}) determined against mouse 3T3 fibroblasts and human transformed liver HepG2 cells using an MTS viability assay.

(D) Comparison of anti-*P. falciparum* (*Pf;* 3D7 strain) and antibacterial activities. Bacteria strains: *E. coli* 25922 (EC), *S. aureus* 27660 (SA), *E. faecalis* 29212 (EF), *P. aeruginosa* 10145 (PA), *K. pneumoniae* 13883 (KP).

(E) Chemical structures of PMX1207 and PMX207. See also Figure S3 and Table S1.

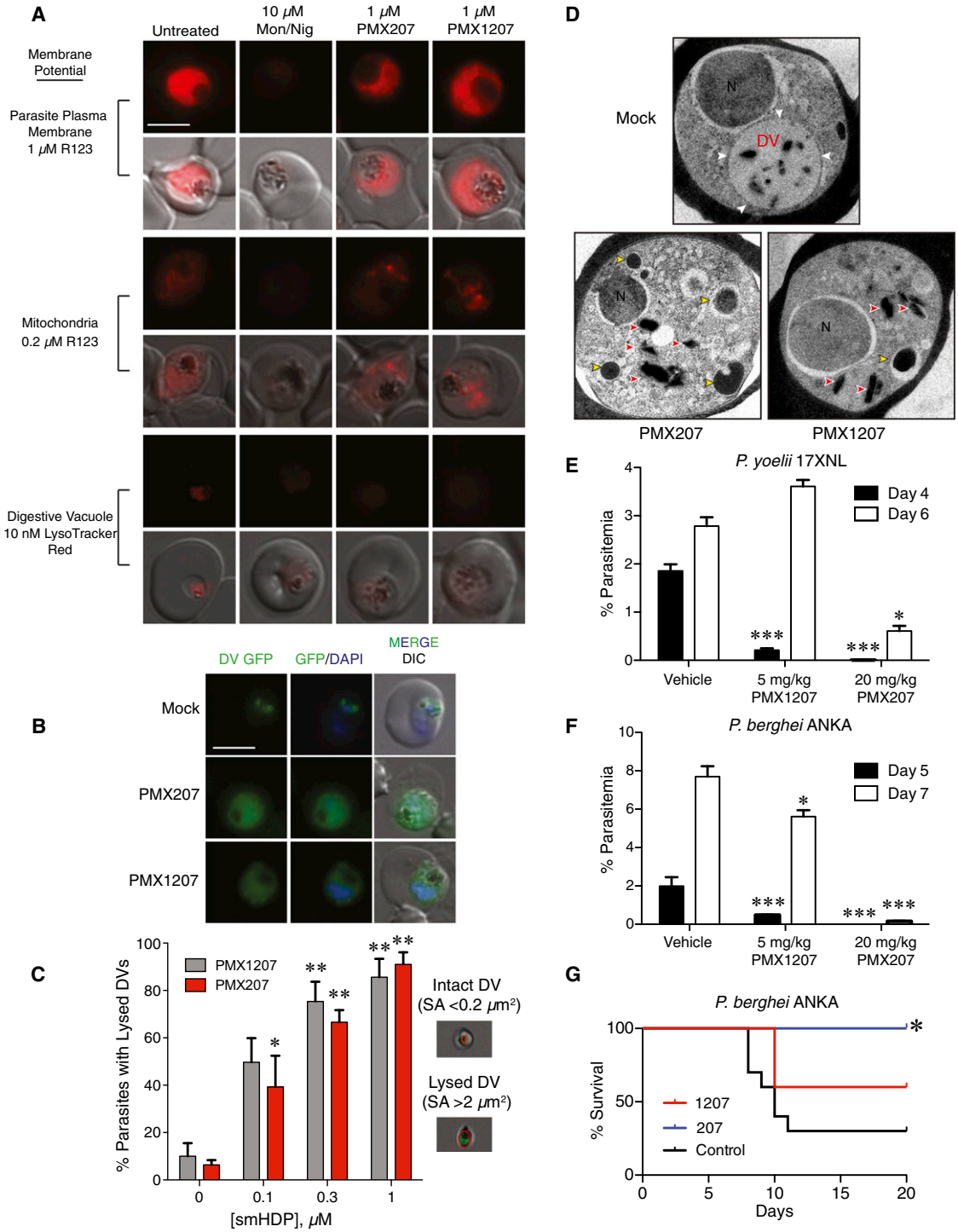

Figure 4. smHDP Leads Kill *P. falciparum* via Parasite DV Lysis and Decrease Parasitemia in a Murine Malaria Model

(A) Parasite plasma membrane and mitochondrial potential was examined during treatment with PMX207 or PMX1207, with no discernible loss of fluorescence, unlike the positive controls. Compromise of DV integrity was monitored with LysoTracker Red, wherein loss of DV fluorescence was seen within 15 min of smHDP treatment, though no loss of parasite plasma membrane potential occurs.

(B) Loss of DV integrity upon smHDP treatment of PM-II-GFP *P. falciparum* parasites (green, PM-II-GFP [DV]; blue, parasite nuclei.)

(C) ImageStream flow cytometry shows a dose-dependent increase in PM-II-GFP parasites showing a fluorescence surface area of >2 μm^2, an indication of DV lysis, upon treatment with PMX207 or PMX1207. Intact DVs have fluorescent surface areas <0.2 μm^2. Data shown are means ± SEM (*$p < 0.05$, **$p < 0.01$).

(D) TEM images reveal complete dissolution of the DV membrane upon PMX207 or PMX1207 treatment, with dispersal of hemozoin crystals (red arrowheads) throughout the cytoplasm and an accumulation of undigested hemoglobin-containing vesicles (yellow arrowheads). Mock-treated parasites retained a clear delineating DV membrane (white arrowheads), encapsulating all hemozoin crystals (N, parasite nucleus).

to limit parasite growth in vivo in both a non-ECM and ECM murine malaria model. PMX207 and PMX1207 antiparasitic activity was assessed using the 4 day Peters' suppression test against *P. yoelii* 17XNL and *P. berghei* ANKA (Figures 4E and 4F). PMX207 completely eliminated parasitemia in both models on days 4 and 5 while PMX1207 showed a significant decrease in parasite growth, suppressing parasitemia at least 5-fold over vehicle-treated controls. Both compounds also increased mouse survival in the ECM model (Figure 4G), with all PMX207 mice surviving through day 20. These data provide in vivo validation that smHDP compounds are a promising class of antimalarials.

DISCUSSION

In this work we show that the human HDP protein, PF4, and its HDP domain alone (C12) kill *Plasmodium* parasites by lysing the parasite DV. Moreover, we screened a library of smHDPs and found molecules that preserved this mechanism of parasite killing while increasing potency. Thus, targeting the lysosome-like vesicles of protozoan parasites may be an evolutionarily selected mechanism for mammalian hosts to kill *Plasmodium* and one that may be exploited for drug discovery. How proteins such as PF4, just the C12 HDP domain of PF4, or smHDPs enter host cells is still an open question and beyond the scope of this work. However, we provide evidence that these molecules enter only infected erythrocytes and that this entry process can be blocked by preincubating with protamine sulfate, a cationic peptide that can also bind to heparin (Figure S1D). This indicates the importance of initial electrostatic interactions with the infected host cell membrane or membrane proteins. Since only infected cells are targeted, and parasite viability is important for uptake, this suggests that a parasite-derived or activated endocytosis-like mechanism could allow for large molecules such as PF4 or C12 to enter, while channels/pores or passive diffusion could be responsible for smHDP uptake.

In closing, human PF4 has the ability to kill blood-stage parasites in vitro, and its low hemolytic potential and selective targeting of the parasite DV endow it with properties that are well tolerated in the bloodstream. However, it is unlikely that PF4 would make a useful therapeutic for malaria treatment due to the cost of goods and potential of increased inflammatory damage during cerebral malaria. Thus, we believe the development of smHDPs may overcome these issues while preserving this unique mechanism of action; thus, smHDPs represent a class of small molecules with effective therapeutic potential for combating this human disease where efforts are currently challenged with rampant drug resistance.

EXPERIMENTAL PROCEDURES

Parasite Culture and IC_{50} Determination

P. falciparum parasites were cultured according to standard conditions (Trager and Jensen, 1976) with minor modifications as outlined in the Supplemental Information. For IC_{50} determinations, compounds were assayed for 72 hr, after which the cultures were fixed with a solution of 4% paraformaldehyde and 0.008% glutaraldehyde in PBS prior to permeabilization with 0.25% Triton X-100 and 5 μM SYTOX Green Nucleic Acid Stain and flow cytometry analysis (Accuri C6 Flow Cytometer with C-Sampler). IC_{50} curves were generated using GraphPad Prism.

Hemolysis

Hemolysis was conducted following removal of culture supernatant before fixing and transferring to a clear-bottom plate. Absorbance at 541 nm was measured and compared to a standard curve generated from Triton X-100-lysed erythrocytes.

Platelet Activation

Platelets were collected from C57BL/6 mice (WT), homozygous PF4 knockout mice (PF4 KO), and transgenic mice overexpressing human PF4 ($hPF4^+$) (Eslin et al., 2004) and added to cultures either with or without preactivation ex vivo with 5 μM AYP. Parasitemia was assessed via flow cytometry after 24 hr treatment.

Parasite Membrane Potential Assays

Parasite-infected erythrocytes were incubated at 37°C for 30 min with 1 μM rhodamine 123 (for parasite plasma membrane potential), 0.2 μM rhodamine 123 (for parasite mitochondrial potential) (del Pilar Crespo et al., 2008), or 10 nM LysoTracker Red (for DV potential). After preincubation, parasites were treated for 4 hr with the test compound, a 10 μM mixture of the ionophores monensin (Sigma) and nigericin (Calbiochem) as a positive control of membrane potential perturbation, or left untreated and then analyzed via fluorescence microscopy on a Leica DMI6000 B.

Fluorescence Microscopy and Quantification of DV Lysis

Erythrocytes infected with synchronous cultures of PM-II-GFP-expressing parasites were treated at 30 hr postinvasion (hpi), fixed at the indicated time points, stained with Hoechst, and imaged by fluorescence microscopy. Cells were also analyzed on an Amnis ImageStream X high-resolution flow cytometer with gating for Hoechst-positive cells to isolate infected cells (Ortyn et al., 2007).

Peptide Synthesis

Peptides were synthesized via standard solid-phase peptide synthesis methods as outlined in detail in the Supplemental Information.

smHDP Screen

Synchronized parasites were treated with 500 nM of each smHDP for 72 hr. Cells were then fixed and assayed for parasitemia via flow cytometry. Compounds were deemed hits if they caused ≥80% parasite death, as compared to a 500 nM chloroquine-treated positive control. The Z factor was calculated using the equation where μ represents the means and σ represents the standard deviations of the positive (p) or negative (n) controls (Zhang et al., 1999).

smHDP Testing in Multiple Parasite, Bacterial, and Mammalian Cell Lines

Synchronized parasite cultures (3D7, NF54;E, Dd2, 7G8, K1, HB3, T2/C6, INDO, V1/S, MT/s1 [MR4, ATCC]) were treated with top smHDP hits for IC_{50} comparison. Titrations for the assay were performed as described previously. Cytotoxicity (EC_{50}) was determined against mouse 3T3 fibroblasts and human transformed liver HepG2 cells using an MTS viability assay. Bacterial MIC determination is outlined in the Supplemental Information.

Transmission Electron Microscopy

Synchronous cultures of *P. falciparum* parasites were treated with either 10 μM PF4, 500 nM PMX207, or PMX1207. DMSO was used as a negative control. A detailed description is provided in the Supplemental Information.

(E) Parasitemias of Swiss Webster mice infected with *P. yoelii* 17XNL parasitized erythrocytes via i.v. injection and treated with vehicle (n = 5), 5 mg/kg PMX1207 (n = 7), or 20 mg/kg of PMX207 (n = 5). Parasitemia was assessed on days 4 and 6. Shown are the means ± SEM (*$p < 0.05$; ***$p < 0.001$).
(F) Parasitemias of C57BL/6 mice infected with *P. berghei* ANKA parasitized erythrocytes via i.v. injection and treated with vehicle (n = 10), 5 mg/kg PMX1207 (n = 5), or 20 mg/kg of PMX207 (n = 5). Parasitemia was assessed on days 5 and 7. Shown are the means ± SEM (*$p < 0.05$; ***$p < 0.001$).
(G) Survival curves for *P. berghei* ANKA infected mice. $p = 0.0189$ in the log rank Mantel-Cox test. See also Figure S4 and Movie S2.

P. berghei ANKA Mouse Studies

C57BL/6 mice were infected with 2.5 × 10^4 *P. berghei* ANKA parasitized erythrocytes via intravenous injection. Mice were dosed once per day intravenously on days 1–4 with either 5 mg/kg PMX1207 (in 20% DMA in saline [n = 5]) or 20 mg/kg PMX207 (in 20% Kleptose HPB [n = 5]) or left untreated (Control, n = 5). Parasitemias were determined on days 5 and 7 via Giemsa-stained blood smears. Mice experiments were performed at Johns Hopkins University (JHU) Bloomberg School of Public Health in accordance with the guidelines of the JHU Institutional Animal Care and Use Committees.

Statistical Analyses

We analyzed the statistical significance of DV lysis with one-tailed paired Student's t tests. Mouse parasitemias were analyzed with a one-way ANOVA with Dunnett's post hoc test. A Mantel-Cox log rank test was performed on the survival data, with a Bonferroni correction for multiple analyses. Significance was assigned to an alpha of 0.01 for DV lysis.

SUPPLEMENTAL INFORMATION

Supplemental Information includes four figures, one table, Supplemental Experimental Procedures, and two movies and can be found with this article online at http://dx.doi.org/10.1016/j.chom.2012.10.017.

ACKNOWLEDGMENTS

We thank Michael Betts, Morgan Reuter, and Johanna Daly for helpful discussions and the following funding sources for this work: NIH R44 AI090762-0 (D.C.G., R.W.S.), NIHT32GM08076 (M.S.L.), NIHT32AI007532 (M.G.M.), NIH R01 AI056840 (P.S.), University of Pennsylvania TAPITMAT Pilot Program (D.C.G.), Penn Genome Frontiers Institute (D.C.G.), and Gates Grand Challenges Exploration Program (D.C.G.).

Received: May 16, 2012
Revised: August 29, 2012
Accepted: October 22, 2012
Published: December 12, 2012

REFERENCES

Bechinger, B. (2009). Rationalizing the membrane interactions of cationic amphipathic antimicrobial peptides by their molecular shape. Current Opinion in Colloid & Interface Science *14*, 349–355.

Christensen, B., Fink, J., Merrifield, R.B., and Mauzerall, D. (1988). Channel-forming properties of cecropins and related model compounds incorporated into planar lipid membranes. Proc. Natl. Acad. Sci. USA *85*, 5072–5076.

del Pilar Crespo, M., Avery, T.D., Hanssen, E., Fox, E., Robinson, T.V., Valente, P., Taylor, D.K., and Tilley, L. (2008). Artemisinin and a series of novel endoperoxide antimalarials exert early effects on digestive vacuole morphology. Antimicrob. Agents Chemother. *52*, 98–109.

Easton, D.M., Nijnik, A., Mayer, M.L., and Hancock, R.E. (2009). Potential of immunomodulatory host defense peptides as novel anti-infectives. Trends Biotechnol. *27*, 582–590.

Eslin, D.E., Zhang, C., Samuels, K.J., Rauova, L., Zhai, L., Niewiarowski, S., Cines, D.B., Poncz, M., and Kowalska, M.A. (2004). Transgenic mice studies demonstrate a role for platelet factor 4 in thrombosis: dissociation between anticoagulant and antithrombotic effect of heparin. Blood *104*, 3173–3180.

Finlay, B.B., and Hancock, R.E. (2004). Can innate immunity be enhanced to treat microbial infections? Nat. Rev. Microbiol. *2*, 497–504.

Gething, P.W., Patil, A.P., Smith, D.L., Guerra, C.A., Elyazar, I.R., Johnston, G.L., Tatem, A.J., and Hay, S.I. (2011). A new world malaria map: Plasmodium falciparum endemicity in 2010. Malar. J. *10*, 378.

Goodier, M.R., Lundqvist, C., Hammarström, M.L., Troye-Blomberg, M., and Langhorne, J. (1995). Cytokine profiles for human V gamma 9+ T cells stimulated by Plasmodium falciparum. Parasite Immunol. *17*, 413–423.

Hancock, R.E., and Lehrer, R. (1998). Cationic peptides: a new source of antibiotics. Trends Biotechnol. *16*, 82–88.

Klemba, M., Beatty, W., Gluzman, I., and Goldberg, D.E. (2004). Trafficking of plasmepsin II to the food vacuole of the malaria parasite Plasmodium falciparum. J. Cell Biol. *164*, 47–56.

Knight, D.J., and Peters, W. (1980). The antimalarial activity of N-benzyloxydihydrotriazines. I. The activity of clociguanil (BRL 50216) against rodent malaria, and studies on its mode of action. Ann. Trop. Med. Parasitol. *74*, 393–404.

Kowalska, M.A., Rauova, L., and Poncz, M. (2010). Role of the platelet chemokine platelet factor 4 (PF4) in hemostasis and thrombosis. Thromb Res. *125*, 292–296.

Ludtke, S., He, K., and Huang, H. (1995). Membrane thinning caused by magainin 2. Biochemistry *34*, 16764–16769.

McMorran, B.J., Marshall, V.M., de Graaf, C., Drysdale, K.E., Shabbar, M., Smyth, G.K., Corbin, J.E., Alexander, W.S., and Foote, S.J. (2009). Platelets kill intraerythrocytic malarial parasites and mediate survival to infection. Science *323*, 797–800.

Moerman, F., Colebunders, B., and D'Alessandro, U. (2003). Thrombocytopenia in African children can predict the severity of malaria caused by Plasmodium falciparum and the prognosis of the disease. Am. J. Trop. Med. Hyg. *68*, 379, author reply 380–381.

Ortyn, W.E., Perry, D.J., Venkatachalam, V., Liang, L., Hall, B.E., Frost, K., and Basiji, D.A. (2007). Extended depth of field imaging for high speed cell analysis. Cytometry A *71*, 215–231.

Pain, A., Ferguson, D.J., Kai, O., Urban, B.C., Lowe, B., Marsh, K., and Roberts, D.J. (2001). Platelet-mediated clumping of Plasmodium falciparum-infected erythrocytes is a common adhesive phenotype and is associated with severe malaria. Proc. Natl. Acad. Sci. USA *98*, 1805–1810.

Scott, R.W., DeGrado, W.F., and Tew, G.N. (2008). De novo designed synthetic mimics of antimicrobial peptides. Curr. Opin. Biotechnol. *19*, 620–627.

Srivastava, K., Cockburn, I.A., Swaim, A., Thompson, L.E., Tripathi, A., Fletcher, C.A., Shirk, E.M., Sun, H., Kowalska, M.A., Fox-Talbot, K., et al. (2008). Platelet factor 4 mediates inflammation in experimental cerebral malaria. Cell Host Microbe *4*, 179–187.

Tang, Y.Q., Yeaman, M.R., and Selsted, M.E. (2002). Antimicrobial peptides from human platelets. Infect. Immun. *70*, 6524–6533.

Tossi, A., Sandri, L., and Giangaspero, A. (2000). Amphipathic, α-helical antimicrobial peptides. Biopolymers *55*, 4–30.

Trager, W., and Jensen, J.B. (1976). Human malaria parasites in continuous culture. Science *193*, 673–675.

Wassmer, S.C., Taylor, T., Maclennan, C.A., Kanjala, M., Mukaka, M., Molyneux, M.E., and Grau, G.E. (2008). Platelet-induced clumping of Plasmodium falciparum-infected erythrocytes from Malawian patients with cerebral malaria-possible modulation in vivo by thrombocytopenia. J. Infect. Dis. *197*, 72–78.

Westerhoff, H.V., Juretić, D., Hendler, R.W., and Zasloff, M. (1989). Magainins and the disruption of membrane-linked free-energy transduction. Proc. Natl. Acad. Sci. USA *86*, 6597–6601.

Yeaman, M.R., Yount, N.Y., Waring, A.J., Gank, K.D., Kupferwasser, D., Wiese, R., Bayer, A.S., and Welch, W.H. (2007). Modular determinants of antimicrobial activity in platelet factor-4 family kinocidins. Biochim. Biophys. Acta *1768*, 609–619.

Zasloff, M. (2002). Antimicrobial peptides of multicellular organisms. Nature *415*, 389–395.

Zhang, J.H., Chung, T.D., and Oldenburg, K.R. (1999). A Simple Statistical Parameter for Use in Evaluation and Validation of High Throughput Screening Assays. J. Biomol. Screen. *4*, 67–73.